**IAEA-CN-77/EXP5/16**

# H-mode Features under ECRH on T-10

Yu.Esipchuk, V.Alikaev, A.Borschegovskij, V.Chistyakov, Yu.Dnestrovskij, M.Dremin, L.Eliseev, S.Grashin, L.Khimchenko, G.Kirnev, N.Kirneva, A.Kislov, D.Kislov, S.Krilov, A.Melnikov, T.Myalton, G.Notkin, Yu.Pavlov, V.Poznyak, I.Roy, D.Shelukhin, S.Soldatov, A.Sushkov, K.Tarasyan, V.Trukhin, E.Trukhina, V.Vershkov

Nuclear Fusion Institute, Russian Research Center "Kurchatov Institute",
123182, Kurchatov Sq., 1, Moscow, Russia

e-mail: esipchuk@nfi.kiae.ru

**Abstract.** The main feature of the H-mode obtained on T-10 under ECRH (with HF power absorbed in the plasma $P_{ab}$ = 0.8 MW) is the spontaneous density $\bar{n}_e$ increase at $D_\alpha$ intensity decrease (up to 4 times). This $\bar{n}_e$ rise is the result of electron transport barrier formation in a narrow region ($\Delta r_H \cong 3$ cm) near the limiter. Confinement enhancement in H-mode up to $Í_L = \tau_E^H/\tau_E^L \cong 1.6\text{-}1.7$ in general is the result of $\tau_A \sim \bar{n}_e$ dependence. The thermal transport barrier contribution to total confinement enhancement is small. Threshold power $P_{th}^{LH}$ does not contradict ITER scaling. Maximal $Í_L$ values are achieved at low $q_L \sim 2.2$, i.e. the dependence $P_{th}^{LH}(q_L)$ exists under T-10 conditions. The results of the radial electric field and turbulence measurements are discussed.

## 1. Introduction

Improved confinement regimes were observed on T-10 under ECRH (*FIG. 1*) in the limiter discharges with circular cross-section ($R_0$=1.5 m, $a_L$=0.3 m). The main properties of these regimes are close to those usually observed in H-mode. L-H bifurcation was obtained in the range of line average density $\bar{n}_e = 1.2 - 2.6 \times 10^{19}\,\mathrm{m}^{-3}$ and plasma current $I_p = 180 - 330$ kA ($q_L$ = 4.1-2.2) both under on-axis ECRH ($B_T$ = 2.42 T) and at ECR zone shift $\Delta R_0$ = 19 cm (off-axis ECRH, $B_T$ = 2.14 T, $r_{ECR}/a_L = 0.65$). The maximal value of HF power absorbed in the plasma was $P_{ab}$ = 0.8 MW (oblique launch, $\psi = 21°$ to the $R_0$ direction, 2nd harmonic, X-mode). The EC current value, $I_{CD}$, in these experiments was small ($I_{CD}/I_p \le 0.1$).

## 2. The Properties of the Improved Confinement Regimes

2.1 L-H bifurcation is shown as a spontaneous density rise (up to 2 times) at the $D_\alpha$ intensity, $I_{D\alpha}$, drop (*FIG. 1*), i.e. at the drop of the particle influx, $\Gamma_{in}^0$, and at the complete switch-off of the gas-puffing valve included in the feedback system. The density increase after bifurcation is accompanied by a plasma stored energy rise ($\beta_p$ on *FIG. 1*). In the best regimes the confinement improvement corresponds to an enhancement factor value of $H_L = \tau_E^H/\tau_E^L \cong 1.6 - 1.7$. Density growth is accompanied by a density gradient increase mainly near the limiter (r/a ≥ 0.8 – *FIG. 2*). This allows us to assume **external** transport barrier formation after bifurcation. But at on-axis ECRH the electron temperature $T_e$ and its profile do not change significantly after bifurcation (*FIG. 3*). This indicates that the thermal transport barrier is small; i.e. the decrease of the thermal transport in the barrier is essentially lower in comparison with the particle transport. Nevertheless the thermal transport barrier forms after bifurcation, because at the ECR zone shift to the plasma periphery (off-axis ECRH) the $T_e$ increase after transition becomes higher, achieving a maximal value at $B_T$ = 2.14 T ($r_{ECR}/a_L = 0.65$, *FIG. 4*). The particle trans-

port barrier plays a general role in confinement improvement while the contribution from the thermal transport barrier to the energy content increase is small. This was confirmed by the experiments in which the density $\bar{n}_e$ in the L-phase was increased up to the same value as in H-mode at the end of the ECRH pulse. The results were expected: the confinement time in L-mode was found to be close to the one in H-mode at the same densities (*FIG. 5*). So, the small decrease of the thermal transport in comparison with the particle transport after bifurcation is the feature of the T-10 improved confinement regime. The other feature of T-10 H-mode is the absence of ELMs in all investigated regimes.

2.2 Plasma potential $\Delta\phi$ behaviour observed by Heavy Ion Beam Probe [1] shows formation of the "potential well" after bifurcation in a narrow region ($\Delta r \cong 3$ cm) near the limiter with the appearance of a "negative" radial electric field ($-\delta E_r$) directed inward (*FIG. 6*). It should be noted that these $\Delta\phi$ values are determined relative to the "base value" in the L-phase (shown on *FIG. 6*). But just at the LH transition the depth of the potential well and the $\delta E_r$ value are small enough and essentially increase ($\delta E_r \cong 400$ V/cm) to the end of the HF pulse with characteristic time about $I_{D\alpha}$ decay time. The potential well and hence the appearance of $\delta E_r$ could take place due to the increased ion losses (after the LH transition) in this region or due to the formation of the electron transport barrier. But as was shown earlier [2] the ion behaviour on T-10 under ECRH ($P_{ab} \cong$ 1-1.5 MW) may be described by $P_{ei}$ changes. This means that under ECRH no additional (turbulent) mechanism of ion transport appears. So it is natural to suppose the formation of a transport barrier for **electrons** after bifurcation.

2.3 The results of turbulence investigations by reflectometry are shown on *FIG. 7*, where the time dependence of the reflection layer radius, $r_{ref}$, is also presented. The amplitude of turbulent fluctuations increases at HF pulse switch-on. The smooth reduction of turbulence amplitude after bifurcation was observed in the frequency range f > 100 kHz when $r_{ref}$ increases (due to density rise) to $r_{ref} \geq 27$ cm. This turbulence reduction takes place in the region where the potential well appears. No turbulence reduction was observed inside of this area (r < 27 cm) and anywhere in the frequency range f < 100 kHz. So these data allow us to assume that the electron transport barrier forms in the region r ≥ 27 cm. The turbulence reduction is smooth with a characteristic time close to that for $I_{D\alpha}$ and $\phi$.

2.4 As the Langmuir probe measurements in the SOL have demonstrated the fast (5-10 ms) drop of $T_e$, ion saturation current $\Gamma_i$ and potential $\phi$ were observed at the LH bifurcation instant [3]. This corresponds to the decrease of $T_e$ and $n_e$ decay length $\lambda$ in the SOL after the transition.

2.5 The following properties of the T-10 improved confinement regime discussed here are also close to those observed in H-mode. The threshold power for LH bifurcation derived from experiments with HF power decrease was found to be $P_{th}^{LH} \cong 0.6$ MW (at on-axis ECRH and $\bar{n}_e = 1.5\times10^{19}\,\mathrm{m}^{-3}$, *FIG. 8,a*). This value is in agreement with ITER scaling [4] $P_{th}^{ITER} = 2.84\cdot M^{-1}\cdot B_T^{0.82}\cdot \bar{n}^{0.58}\cdot R\cdot a^{0.81}$. So at maximal HF power the total heating power value $P_{tot} \approx 1.7\cdot P_{th}^{LH}$. If the initial density $\bar{n}_e$ increases, the $H_L$ value decreases. This corresponds to $P_{th}^{LH}$ rise with $\bar{n}_e$ (*FIG. 8,b*). The $\bar{n}_e$ value at which LH bifurcation is not observed (i.e. $P_{th}^{LH} = P_{tot}$) is in agreement with that expected in accordance with ITER scaling (vertical line on *FIG. 8,b*). But investigation has shown that $H_L$ dependence on $q_L$ is a feature of the T-10

improved confinement regime (*FIG. 8,c*). The highest $H_L$ value was achieved at low $q_L \cong 2.2$. $H_L$ decreases with $q_L$ rise and LH bifurcation does not exist at $q_L \geq 4.1$. One can relate this $P_{th}^{LH}(q_L)$ dependence to $\nabla T_e$ decrease due to the $T_e(r)$ peaking with $q_L$ increase.

### 3. Discussion

The smooth increase of potential well depth (near the limiter) and turbulence amplitude decrease with a characteristic time close to that for the $I_{D\alpha}$ drop allow us to suppose that the electron transport barrier arising at $t_{LH}$ continues to become deeper (i.e. the electron transport in the barrier continues to decrease) up to the steady state of the H-phase. This was confirmed by the results of modelling, according to which the value of $D_e^H / D_e^L$ in the barrier is about $1/2 - 1/3$ and decreases to $D_e^H / D_e^L \cong 1/5 - 1/6$ at the end of the HF pulse. On the basis of these data one can also make the following supposition. A) To explain the LH transition the condition $\frac{1}{r}\frac{d}{dr}(E \times B) > \gamma$, (1) is often used, i.e. the E×B velocity shear becomes great enough to exceed the growth rate of turbulent fluctuations γ. But condition (1) means that turbulence should be completely suppressed and the transport barrier should form just at the LH transition. So condition (1) is not completely adequate for the phenomena observed on T-10. B) Continuing changes of $\delta E_r$ (up to 400 V/cm) and changes in turbulence amplitude after the LH transition up to the H-phase steady state allow us to assume the existence of the following feedback mechanism: a relatively small radial electric field $\delta E_r$ arising at the LH instant leads to the increase of E×B velocity shear, partial stabilisation of turbulence and, hence, decrease of electron transport. It results, in turn, in $\delta E_r$ increase and so this feedback loop is closed. This process continues up to steady state conditions, which determines the final depth of the potential well and electron transport barrier.

The results obtained in the T-10 improved confinement regimes qualitatively agree with the conclusions of theory [5]. According to this theory the increase of turbulence and electron transport after HF pulse switch-on results in poloidal velocity $V_p$ generation, which influences the stabilising effect on the turbulence. When the $V_p$ achieves some threshold value $(V_p)_{th}$ this effect becomes dominant, which leads to turbulence and electron transport decrease. This is the LH transition. According to [5] after the LH transition the stabilisation can continue, which also does not contradict to experimental data. If this is so, the turbulence itself can be considered as the trigger of the LH transition. To examine this supposition modelling of the T-10 regimes discussed above using the theory of [5] is now in progress.

This work is supported by Minatom of Russia (contract 105F) and by the Russian Ministry of Science and Technology (Federal Program “Contr. Therm. Fusion and Plasma Processes”).

[1] MELNIKOV, A.V., et al., 1999, 26 EPS Conf. Plasma Phys. Control Fusion, Maastricht, 23J, p. 829
[2] ALIKAEV, V.V., et al., 1985, Proc. of 12th Conf. Plasma Physics and Contr. Nucl. Fus., London, v.1 (Vienna: IAEA), p.419
[3] KIRNEV, G.S., GRASHIN, S.A., KHIMCHENKO, L.N., will be published in Czechoslovak Journal of Physics, 2000,Vol. 50, No 12.
[4] Technical Basis for the ITER-FEAT Outline Design, Ch. 1, Sec. 2, p. 3
[5] DNESTROVSKII, Yu.N., OSIPENKO, M.V., TSAUN, S.V., Fizika Plasmy, 1998, v.24, No. 9, p.771.

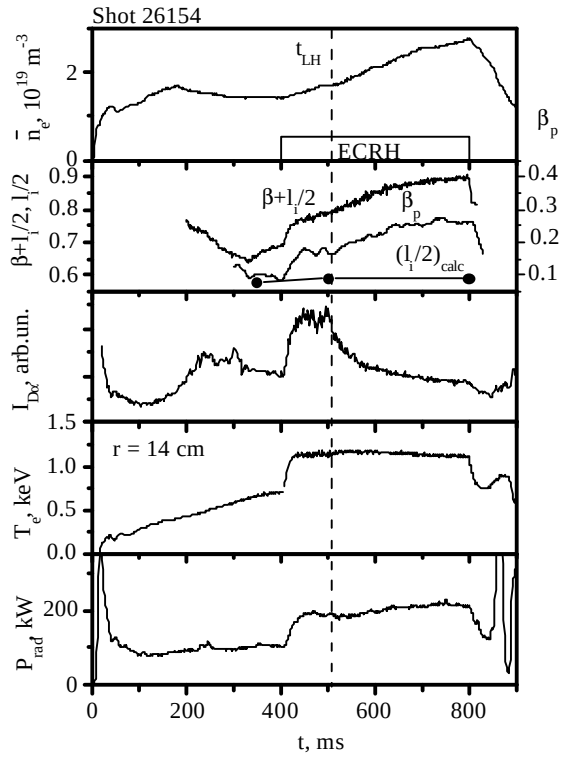


*FIG. 1 Traces of $\bar{n}_e$, $b_p+l_i/2$, $b_p$ (diamagnetic measurements), $I_{Da}$, $T_e$(14 cm) and $P_{rad}$ (radiative losses). $t_{LH}$- the instant of the L-H transition. $B_T$=2.42 T (on-axis), $q_L$=2.2, $P_{ab}$=0.8 MW.*

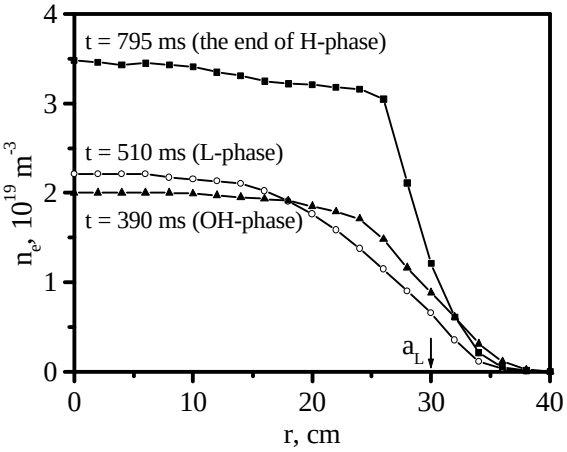


*FIG. 2 Density profiles for OH, L- and H-phases. $B_T$=2.42 T (on-axis), $q_L$=2.2, $P_{ab}$=0.8 MW.*

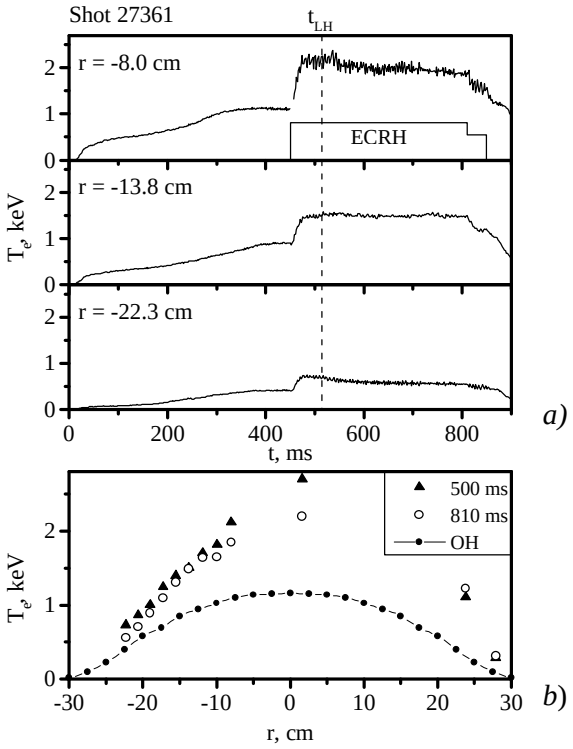


*FIG. 3 (a)-Traces of $T_e$(r). (b)- $T_e$ profiles for OH-, L-(t=500 ms) and H-(t=810 ms) phases. $B_T$=2.42 T (on-axis), $q_L$=2.2, $P_{ab}$=0.8 MW.*

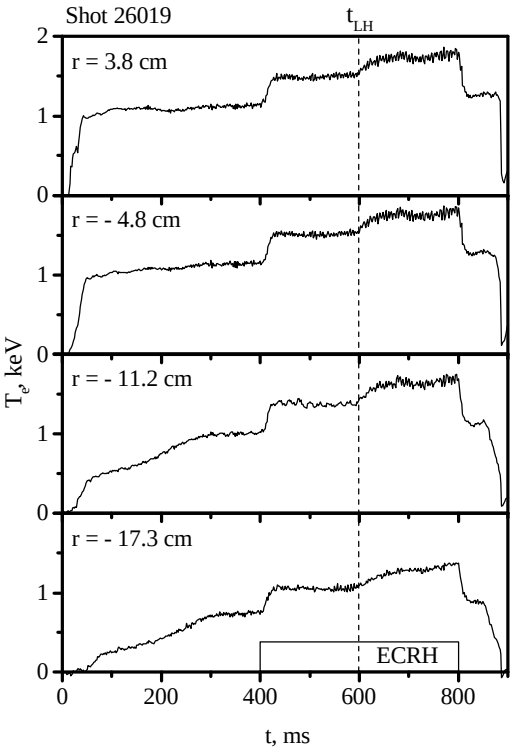


*FIG. 4 Traces of $T_e$ in the regime with off-axis ECRH.*

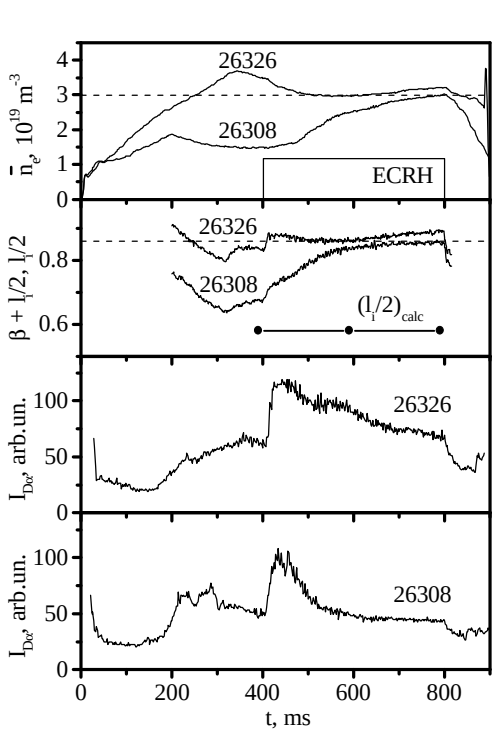


*FIG. 5 Traces of $\bar{n}_e$, $b_p+l_i/2$ and $I_{Da}$ in shots with the same density $\bar{n}_e$ in the L-phase (26326) and at the end of the H-phase (26308). $B_T$=2.42 T (on-axis), $q_L$=2.2, $P_{ab}$=0.8 MW.*

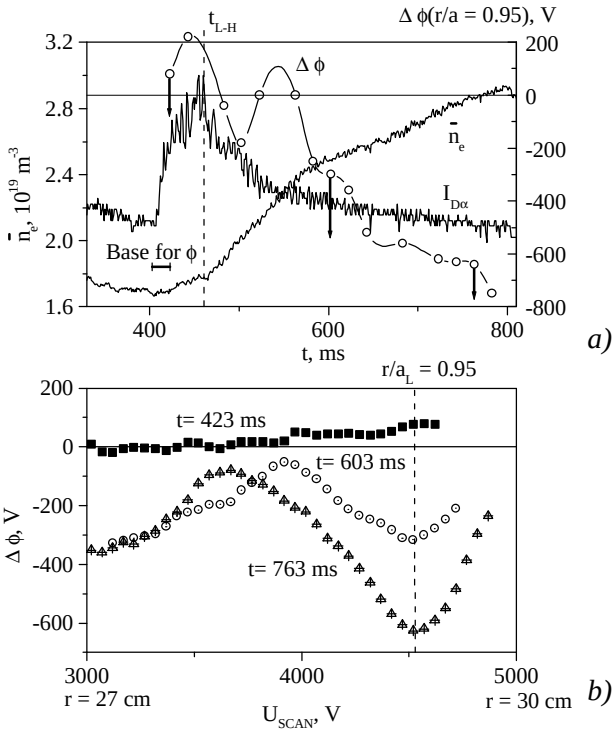


*FIG. 6 (a) Plasma potential Df behaviour in comparison with $\bar{n}_e$ and $I_{Da}$ ; (b) profiles of plasma potential at instants marked by arrows on FIG 6(a). $B_T$=2.42 T (on-axis), $q_L$=2.2, $P_{ab}$=0.8 MW.*

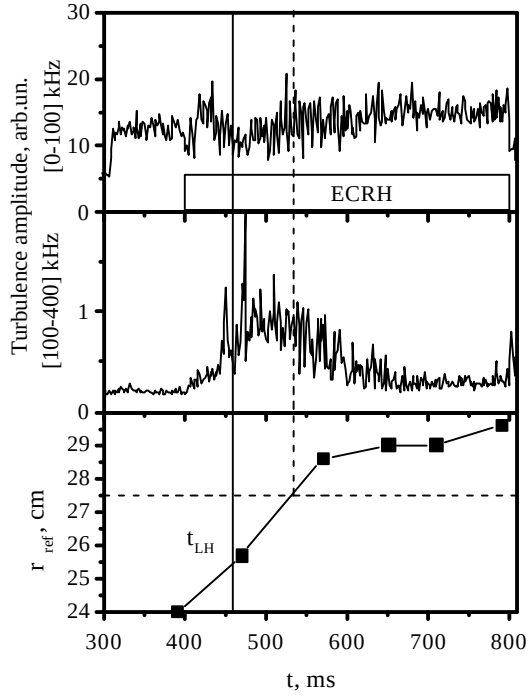


*FIG. 7 Turbulence amplitude behaviour in two frequency ranges. $B_T$=2.42 T (on-axis), $q_L$=2.2, $P_{ab}$=0.8 MW. Time behaviour of the reflection layer radius $r_{ref}$ is shown.*

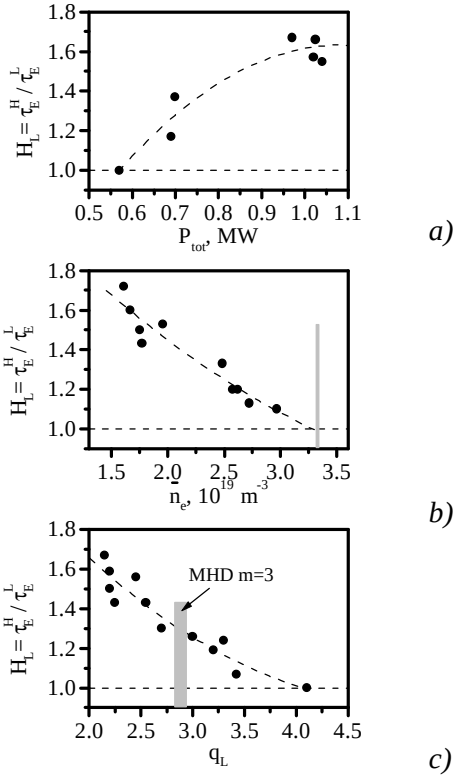


*FIG. 8 $H_L$ dependencies on $P_{tot}$(a), $\bar{n}_e$(b), $q_L$ (c). On-axis ECRH.*